# Stability Analysis and Convergence Control of Iterative Algorithms for Reliability Analysis and Design Optimization

**Dixiong Yang**[1]
Associate Professor
e-mail: yangdx@dlut.edu.cn

**Hui Xiao**
e-mail: vihuixiao@163.com

Department of Engineering Mechanics,
Dalian University of Technology,
State Key Laboratory of Structural Analysis
for Industrial Equipment,
Dalian 116023, China

*Iterative algorithms are widely applied in reliability analysis and design optimization. Nevertheless, phenomena of failed convergence, such as periodic oscillation, bifurcation, and chaos, are oftentimes observed in iterative procedures of solving some nonlinear problems. In the present paper, the essential causes of numerical instabilities including periodic oscillation and chaos of iterative solutions are revealed by the eigenvalue-based stability analysis of iterative schemes. To understand and control these instabilities, the stability transformation method (STM), which is capable of tackling numerical instabilities of iterative algorithms in reliability analysis and design optimization, is proposed. Finally, several benchmark examples of convergence control of PMA (performance measure approach) for probabilistic analysis and the SORA (sequential optimization and reliability assessment) for reliability-based design optimization (RBDO) are presented. The observations from the benchmark examples indicate that the STM is a promising approach to achieve convergence control for iterative algorithms in reliability analysis and design optimization.* [DOI: 10.1115/1.4023327]

*Keywords: reliability analysis and optimization, iterative algorithms, numerical instabilities, chaotic dynamics, stability transformation method, convergence control*

## 1 Introduction

In practice, most problems of interest in structural and mechanical systems exhibit nonlinear behavior. At present, iterative approaches are popular for solving nonlinear analysis and design problems of engineered systems. As they are easy to understand and convenient to run, iterative methods are widely used in engineering practice. For some nonlinear systems, however, iterative methods cannot acquire convergent solutions (namely, fixed point solutions). In some cases, iterative methods only obtain oscillating periodic solutions (i.e., they fall into cycling with certain period), while in others they obtain chaotic solutions (theoretically, infinite periodic solutions within a specific region) with pseudorandomness and disorder. Unfortunately, in the fields of computational mechanics and engineering, many researchers lack the knowledge that reveals inherent mechanisms of complicated phenomena such as oscillation and chaos in numerical solutions of iterative equations, and have very limited insights on how to control their convergent behavior and capture desired fixed points (i.e., period-1 solutions).

Recently, Yang and his colleagues [1–6] investigated essential reasons of iterative failure of some popular algorithms used in reliability analysis, design optimization, and other fields. The popular algorithms explored were FORM (first order reliability method), PMA, SAP (sequential approximate programming) with PMA based probabilistic optimization, convex approximation optimization (e.g., the convex linearization method and the method of moving asymptotes), and the capacity spectrum method for structural seismic analysis. Furthermore, they suggested a set of convergence control strategies for these iterative algorithms from a new perspective of nonlinear dynamics.

Actually, chaotic dynamics theory [7–10] is a powerful tool for comprehensively understanding complicated phenomena of numerical instabilities, and controlling convergence failure of iterative methods. The iterative procedure of a nonlinear system forms a nonlinear map, i.e., $\mathbf{x}_{k+1}=\mathbf{f}(\mathbf{x}_k)$; this nonlinear map can be viewed a discrete dynamical system. When the spectral radius of the Jacobian matrix of a dynamical system at a fixed point is larger than 1, its solution can yield numerical instabilities of divergence (i.e., the solution tends to infinite), periodic oscillation, bifurcation (the state of solution changes, e.g., periodic doubling bifurcation refers to a solution from a fixed point to period-2 point and to period-4 point, etc.), and chaos in the specific parameter interval. Otherwise, when the spectral radius of the Jacobian matrix of a dynamical system is less than 1, a stable and convergent solution arises [9]. The stability analysis of fixed point solutions is of significance in grasping evolutional behaviors of nonlinear dynamical systems, see [8–10] for details.

In recent years, RBDO has been of great interest in the field of structural and mechanical engineering [11,12]. The numerical approaches for RBDO are classified into three categories according to the type of iterative formulations: two-level approaches, monolevel approaches, and decoupled approaches. Specifically, two-level approaches consist of two loops. The outer loop performs the cost optimization, and the inner loop assesses reliability constraints. Monolevel approaches are also called single loop approaches as they solve RBDO problems in a single loop procedure to avoid the explicit reliability analysis. The third type of numerical solution technique, decoupled approaches, separate reliability analysis from the optimization procedure [11,12]. The SORA method is one such decoupled approach with reasonable computational demand for complex structural systems [11,13]. SORA, however, may suffer from the aforementioned numerical instability challenges on some occasions.

This paper first reveals fundamental causes for iterative failure based on the stability analysis of the Jacobian matrix of iterative systems. Furthermore, based upon the principle of chaos control, the STM is proposed to control periodic oscillation, bifurcation, and chaos of iterative schemes for reliability analysis and optimization. The STM method also finds stable convergent solutions. Moreover, STM is suggested to conquer the nonconvergence issue of PMA for probabilistic analysis and SORA. To warrant these claims, several illustrative examples are studied. The stability analysis of fixed point of the nonlinear iterative map derived from PMA and convergence control for SORA using STM are the main contributions of this work.

## 2 Numerical Instabilities of Iterative Algorithms in Reliability Analysis and Design Optimization

The nonlinear map derived from iterative algorithms in reliability analysis and optimization can be generally expressed as an $n$-dimensional discrete dynamical system

$$\mathbf{x}_{k+1}=\mathbf{f}(\mathbf{x}_k,\mathbf{p}) \tag{1}$$

[1]Corresponding author.

Contributed by the Design Automation Committee of ASME for publication in the Journal of Mechanical Design. Manuscript received January 14, 2011; final manuscript received December 12, 2012; published online January 17, 2013. Assoc. Editor: Wei Chen.

  

in which $k$ denotes the $k$th iteration, the iterative function vector $\mathbf{f}$ is differentiable, $\mathbf{x}$ is a $n \times 1$ dimensional state vector, and $\mathbf{p}$ is a vector of control parameters of the dynamical system. This dynamical system has an explicit or implicit expression according to a specific problem to be solved. Sometimes, it is difficult to determine the control parameters in complicated systems. In the HL-RF algorithm of FORM [14–17] and the AMV (advanced mean value) formula of PMA [18–22], the mean value $\mu$ or the standard deviation $\sigma$ of random variables can be regarded as control parameters of nonlinear maps.

Even for a very simple nonlinear map like the Logistic map $x_{k+1} = f(x_k, r) = rx_k(1 - x_k)$, where $r$ is a control parameter with $1 \le r \le 4$, the evolutionary dynamics behavior is quite complex with iterative solutions that may exhibit periodic oscillation, bifurcation, and chaos for certain control parameter intervals [7–10]. The Logistic map is a typical nonlinear dynamical model often used to describe the growth of biological populations [1,7–9].

For iterative algorithms, like dynamical systems, numerical stability depends on the mathematical form of the nonlinear map. If the spectral radius (i.e., the maximum of the absolute value of the eigenvalues) of the Jacobian matrix $\mathbf{J}$ ($\mathbf{J} = \partial \mathbf{f}_i / \partial \mathbf{x}_j |_{\mathbf{x}_f}$) of a dynamical system (1) at the fixed point $\mathbf{x}_f$ is larger than 1, namely, $\rho(\mathbf{J}) > 1$, the fixed point will lose its stability in the specific parameter interval and repel future iterations of the iterative scheme. This repellant behavior leads to stability and convergence issues like periodic oscillation, bifurcation, and chaos. On the other hand, if the spectral radius of the Jacobian matrix of dynamical system (1) is smaller than 1 ($\rho(\mathbf{J}) < 1$), the fixed point $\mathbf{x}_f$ is attractive and a stable, convergent solution is obtained. If $\rho(\mathbf{J}) = 1$, the stability of the iterative solution is indefinite and may be attractive or repellant [9]. The detailed examples of stability analysis for iterative maps from practical application are shown in Secs. 3 and 4.

The above stability conditions of iterative systems indicate that when one uses iterative algorithms for engineering computations, or when one attempts to prove the convergence of iterative algorithms, it is necessary to take both the existence and stability of fixed points into account.

## 3 Stability Transformation Method for Convergence Control of Iterative Algorithms

As pointed out in Sec. 2, an iterative dynamical system (1) could lose stability of fixed points and produce undesired periodic and chaotic solutions. The character of stability and convergence theoretically depend on the spectral radius $\rho(\mathbf{J})$ of Jacobian matrix of dynamical system $\mathbf{x}_{k+1} = \mathbf{f}(\mathbf{x}_k, \mathbf{p})$. An illustrated example of the Henon nonlinear map is displayed later to demonstrate this concept. Numerical analysis demonstrates how the spectral radius $\rho(\mathbf{J})$ of system affects the stability of fixed points and convergence of solutions.

Fortunately, chaos feedback control can catch desired fixed points embedded in the chaotic attractor of nonlinear dynamical system through implementing the target guidance and position. Feedback control can also stabilize unstable fixed points involved in the periodic orbit of dynamical systems, and control oscillation and bifurcation [8,23,24].

Schmelcher and Diakonos [23] introduced an appropriate linear transformation to modify the eigenvalues of Jacobian matrix of original dynamical systems (1) and stabilize unstable fixed points of original systems without changing their values and locations. This method is referred to the stability transformation method [24], whose expression is

$$\mathbf{x}_{k+1} = \mathbf{x}_k + q\mathbf{C}[\mathbf{f}(\mathbf{x}_k, \mathbf{p}) - \mathbf{x}_k] \tag{2}$$

in which, $0 < q < 1$, $\mathbf{C}$ is the $n \times n$ dimensional involutory matrix. In this matrix, only one element in each row and each column in this matrix is 1 or $-1$, and the others are 0. The total number of permissible involutory matrices is $2^n n!$, and $\mathbf{C}$ is an orthogonal matrix.

The Jacobian matrix $\bar{\mathbf{J}}$ of the STM scheme (2) is formulated as

$$\bar{\mathbf{J}} = \mathbf{I} + q\mathbf{C}(\mathbf{J} - \mathbf{I}) \tag{3}$$

Theoretically, the factor $q$ and involutory matrix $\mathbf{C}$ can be chosen to make the spectral radius of Jacobian matrix of STM equation less than 1 ($\rho(\bar{\mathbf{J}}) < 1$) and thus achieve stable convergence. In general, the selection of involutory matrix $\mathbf{C}$ in Eq. (2) relies on the original system's properties. To enhance the efficiency of stabilizing the periodic orbit, it is unnecessary to take all the $2^n n!$ involutory matrices, but it is desirable to select the minimum set of these matrices. Usually, selecting the identity matrix for $\mathbf{C}$ can stabilize the unstable fixed point of the chaotic dynamical system. Moreover, selection of the factor $q$ is closely dependent on the spectral radius of the original system's Jacobian matrix at the fixed point. The larger the spectral radius of the Jacobian matrix of the original dynamical system, the smaller the factor $q$ should be taken to achieve stabilization. Smaller values of $q$ lead to a larger number of iterations required to obtain convergent solutions [2–5]. When $\mathbf{C} = \mathbf{I}$ ($\mathbf{I}$ is the identity matrix), Eq. (2) becomes

$$\mathbf{x}_{k+1} = \mathbf{x}_k + q[\mathbf{f}(\mathbf{x}_k, \mathbf{p}) - \mathbf{x}_k] \tag{4}$$

where if $q = 1$ the original dynamic system is not controlled. The advantages and limitations of STM are clarified in Refs. [2–5]. Overall, STM is an effective, simple and versatile approach to realize the control of periodic oscillation, bifurcation, and chaos of dynamical systems.

Finally, one representative nonlinear iterative map, the Henon map [8,9], is presented as an example to illustrate complicated dynamical behavior, instability analysis and convergence control by STM. The nonconvergence phenomena and convergence control of PMA for probabilistic analysis and SORA for RBDO will be presented in Secs. 4 and 5. In 1976, Henon constructed this map from an astronomical model. The Henon map can be obtained through superimposing three simple maps [8,9].

*Example 1:* Henon map [8,9]

$$\begin{cases} x_{k+1} = a - x_k^2 + by_k \\ y_{k+1} = x_k \end{cases} \tag{5}$$

in which $b$ is a parameter, and $a$ is the control parameter of the dynamical system. Usually, $b = 0.3$ and $0 \le a \le 1.4$.

If the Henon map has fixed points, then $x_{k+1} = x_k = x_f$, $y_{k+1} = y_k = y_f$. Substituting them into Eq. (5) shows the fixed points of the Henon map are

$$\begin{cases} x_f = \left[b - 1 \pm \sqrt{(b-1)^2 + 4a}\right] \Big/ 2 \\ y_f = x_f \end{cases} \tag{6}$$

The Jacobian matrix of the Henon map is written as

$$\mathbf{J} = \begin{bmatrix} \dfrac{\partial x_{k+1}}{\partial x_k} & \dfrac{\partial x_{k+1}}{\partial y_k} \\ \dfrac{\partial y_{k+1}}{\partial x_k} & \dfrac{\partial y_{k+1}}{\partial y_k} \end{bmatrix} = \begin{bmatrix} -2x_k & b \\ 1 & 0 \end{bmatrix} \tag{7}$$

Further, the eigenvalues of Jacobian matrix of the Henon map at one fixed point are

$$\lambda_{1,2} = -x_f \pm \sqrt{x_f^2 + b} \tag{8}$$

Figure 1 shows the two eigenvalues of the Henon map corresponding to the larger fixed point changing with the control parameter $a$. It is seen that the larger eigenvalue $\lambda_1$ is always less than 1. While the absolute value of smaller eigenvalue $\lambda_2$ is less

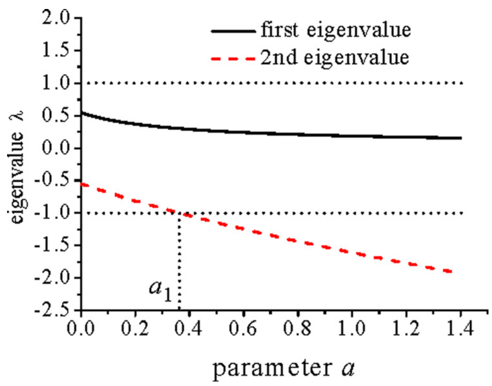


**Fig. 1 Eigenvalues of the Henon map at larger fixed point**

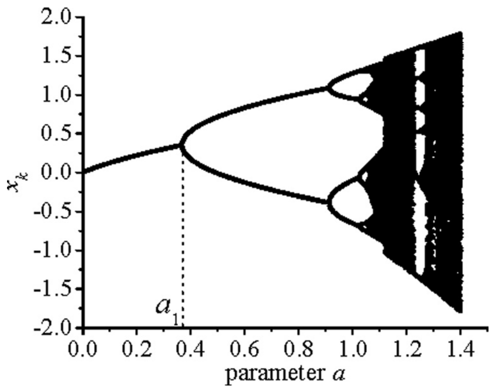


**Fig. 2 Bifurcation plot of the Henon map**

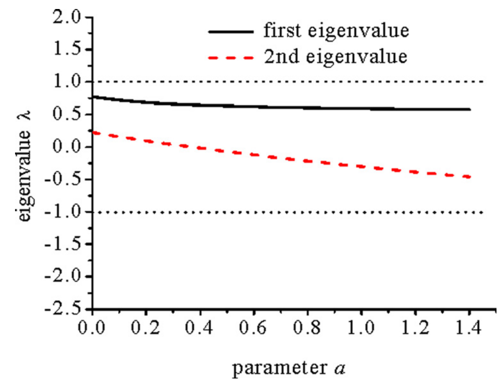


**Fig. 3 Eigenvalues of STM scheme of the Henon map**

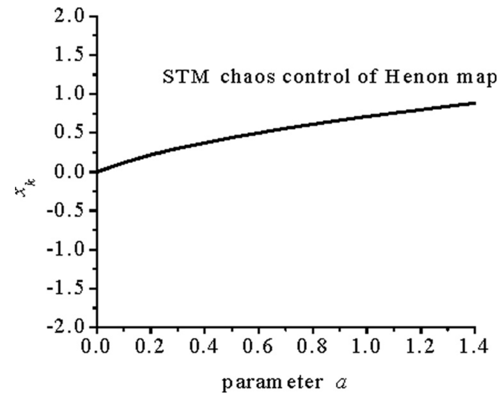


**Fig. 4 STM chaos control of the Henon map**

than 1 when $a < a_1$ ($a_1 = 0.3675$ corresponding to the first bifurcation point of bifurcation plot), and greater than 1 when $a > a_1$. Consequently, in accordance with the stability conditions of fixed points of nonlinear iterative map presented in Sec. 2, only in the interval [0, $a_1$) is the larger fixed point of the Henon map a trivial attractor. When $a > a_1$, the fixed point becomes an unstable saddle point, and periodic/chaotic solutions emerge in the dynamical system. Figure 2 demonstrates the corresponding bifurcation plot of the Henon map with varying parameter $a$, which presents the state of iterative solutions in good agreement with that of stability analysis.

To overcome the nonconvergence, according to Eq. (2) the iterative scheme of the Henon map using STM ($\mathbf{C} = \mathbf{I}$) is altered as

$$\begin{cases} x_{k+1} = q(a - x_k^2 + by_k) + (1-q)x_k \\ y_{k+1} = qx_k + (1-q)y_k \end{cases} \tag{9}$$

The fixed points of STM scheme of the Henon map are then expressed as

$$\begin{cases} x_f = \left[b - 1 \pm \sqrt{(b-1)^2 + 4a}\right] \Big/ 2 \\ y_f = x_f \end{cases} \tag{10}$$

This verifies that the STM scheme does not change the value of fixed points of original dynamical system. In terms of Eq. (3) the Jacobian matrix $\bar{\mathbf{J}}$ of the STM scheme for the Henon map is written as

$$\bar{\mathbf{J}} = \mathbf{I} + q(\mathbf{J} - \mathbf{I}) = \begin{bmatrix} 1 - q - 2qx_k & qb \\ q & 1 - q \end{bmatrix} \tag{11}$$

Accordingly, the two eigenvalues $\lambda'_{1,2}$ of Jacobian matrix in the STM scheme of the Henon map at one fixed point are obtained

$$\lambda'_{1,2} = 1 - q + q\lambda_{1,2} = 1 - q - qx_f \pm q\sqrt{x_f^2 + b} \tag{12}$$

When $q = 0.5$, then $\lambda'_{1,2} = 0.5 - 0.5x_f \pm 0.5\sqrt{x_f^2 + b}$.

Two eigenvalues of the STM scheme for the Henon map at the larger fixed point, as a function of control parameter $a$, are shown in Fig. 3 ($q = 0.5$). It is observed that the absolute values of two eigenvalues $\lambda'_{1,2}$ are less than 1 in the interval [0,1.4] of parameter $a$. Hence, the Henon map controlled by STM ($q = 0.5$) always has a trivial attractor on this interval, and the unstable fixed point of the original Henon map is stabilized as displayed in Fig. 4.

Figure 5 illustrates the iterative history of the $x$ component of the Henon map ($b = 0.3$, $a = 1.4$). It is observed that the chaotic solutions of the Henon map emerge. The iterative history for the Henon map that uses STM ($\mathbf{C} = \mathbf{I}$, $q = 0.5$) for chaos control ($b = 0.3$, $a = 1.4$) is shown in Fig. 6. After 16 iterations, the STM scheme of the Henon map captures the expected fixed point.

## 4 Convergence Control of PMA for Probabilistic Analysis

Probabilistic analysis of performance functions is an important task in uncertainty propagation for stochastic systems. It is desirable to obtain cumulative distribution functions (CDF) and probability density functions (PDF) of system responses since these functions contain complete probabilistic information about them.

As a method of inverse reliability analysis, PMA can calculate the CDF and PDF of performance functions more efficiently than numerical simulation approaches such as Monte Carlo simulation

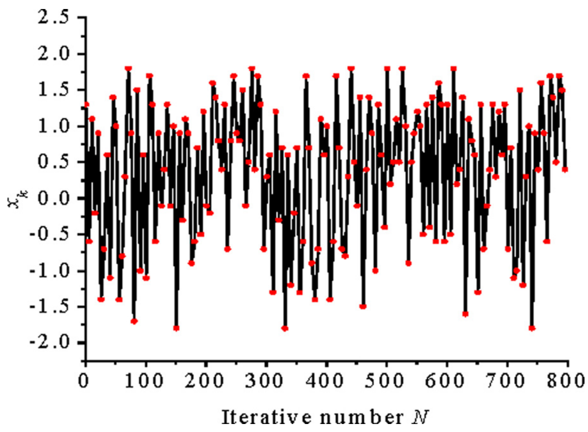


**Fig. 5 Iterative history of the Henon map**

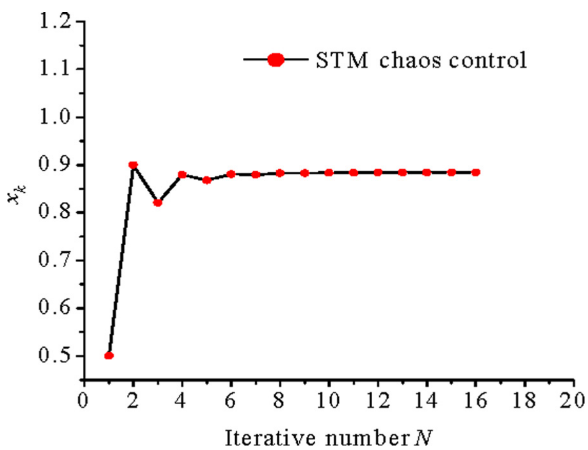


**Fig. 6 Iterative history of STM scheme of the Henon map**

(MCS), importance Monte Carlo simulation, and so on. The specific procedure of PMA to compute CDF and PDF may be found in Refs. [21,25]. However, if the advanced mean value scheme (13) of PMA is employed to solve for the CDF, it will not converge due to numerical instability [21,25]. Therefore, the STM scheme (14) for convergence control of PMA is activated and used to alter the original AMV formula, which is written in a standard normal space as

$$\mathbf{u}_{k+1} = -\beta_t \frac{\nabla g(\mathbf{u}_k)}{\|\nabla g(\mathbf{u}_k)\|} \tag{13}$$

$$\mathbf{u}_{k+1} = \mathbf{u}_k + q\mathbf{C}\left(-\beta_t \frac{\nabla g(\mathbf{u}_k)}{\|\nabla g(\mathbf{u}_k)\|} - \mathbf{u}_k\right) \tag{14}$$

where $\mathbf{u}$ is the standard normal variable vector, $\beta_t$ represents the target reliability index, and $g(\mathbf{u}_k)$ is the performance function. For general cases, the involutory matrix $\mathbf{C}$ is taken as the identity matrix, and the factor $q$ can be set as 0.5, 0.1, or some smaller value in sequence to balance its stabilizing effect on the system with its computational cost [2–6]. Indeed, the factor $q$ cannot be automatically predefined for complicated implicit maps from iterative algorithms because the spectral radius of Jacobian matrix of complex implicit maps at fixed points are not known beforehand. Since the spectral radius determines the stability of the STM scheme (14) and hence affects the magnitude of $q$, $q$ cannot be known exactly at the onset of the calculation. This is a common feature of other approaches (e.g., the relaxation method, move limits, moving asymptotes and trust region management) of convergence control that also involve some parameters which cannot be set in advance, as pointed out in Ref. [5]. STM has a solid mathematical basis and is a promising control strategy for attacking nonconvergence problems of iterative computation in probabilistic analysis and optimization design [2–5].

*Example 2:* Probabilistic analysis of the performance function [3,19]

$$g(\mathbf{x}) = [\exp(0.8x_1 - 1.2) + \exp(0.7x_2 - 0.6) - 5]/10,$$
$$x_1 \sim \mathrm{N}(4, 0.8), \quad x_2 \sim \mathrm{N}(5, 0.8)$$

When using the AMV iterative formula (13) to search for the MPTP (minimum performance target point) of performance function in example 2 with target reliability index $\beta_t \in [-3, 3]$, periodic solutions arise in the interval [2.618, 3] as shown in Figs. 7(*a*) and 7(*b*). Figure 7(*b*) is the zoomed in view of Fig. 7(*a*) to make the bifurcation behavior clear.

Subsequently, the stability analysis of the AMV formula for solving example 2 is carried out. The explicit iterative scheme of AMV formula (13) for example 2 is expressed as

$$\begin{cases} u_1^{k+1} = -\beta_t \dfrac{0.064\exp(0.64u_1^k + 2)}{\sqrt{(0.064\exp(0.64u_1^k + 2))^2 + (0.056\exp(0.64u_2^k + 2.9))^2}} \\ u_2^{k+1} = -\beta_t \dfrac{0.056\exp(0.64u_2^k + 2.9)}{\sqrt{(0.064\exp(0.64u_1^k + 2))^2 + (0.056\exp(0.64u_2^k + 2.9))^2}} \end{cases} \tag{15}$$

The corresponding Jacobian Matrix can be written as

$$\mathbf{J} = \begin{bmatrix} \dfrac{\partial u_1^{k+1}}{\partial u_1^k} & \dfrac{\partial u_1^{k+1}}{\partial u_2^k} \\ \dfrac{\partial u_2^{k+1}}{\partial u_1^k} & \dfrac{\partial u_2^{k+1}}{\partial u_2^k} \end{bmatrix} = \begin{bmatrix} J_{11} & J_{12} \\ J_{21} & J_{22} \end{bmatrix} \tag{16}$$

The first eigenvalue $\lambda_1$ at the fixed point has a complicated expression not shown here, and the second eigenvalue at the fixed point $\lambda_2 = 0$. It is noted that Eq. (15) is decoupled for two variables, and $\det(\mathbf{J}) = 0$ in Eq. (16) implies that the eigenvalue $\lambda_2$ of $\mathbf{J}$ should be equal to zero. Figure 8 exhibits the two eigenvalues of AMV scheme (13) at the fixed point changing with parameter $\beta_t$. It is observed that the absolute value of the first egienvalue $\lambda_1$ is less than 1 when $\beta_t < 2.618$, and greater than 1 when $\beta_t > 2.618$. Therefore, only in the interval [0, 2.618) is the fixed point of the AMV scheme stable.

Furthermore, the convergence control of AMV formula by STM is performed. According to Eq. (14) the STM scheme ($\mathbf{C} = \mathbf{I}$, $q = 0.5$) is described as

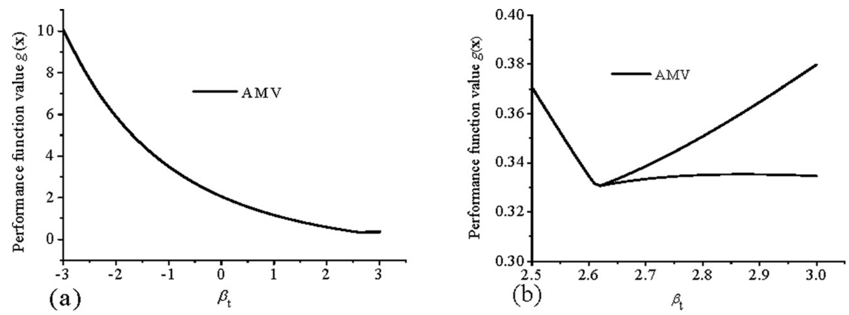


**Fig. 7** (*a*) **Bifurcation plot of the AMV formula and** (*b*) **Local zooming view of bifurcation plot of the AMV formula**

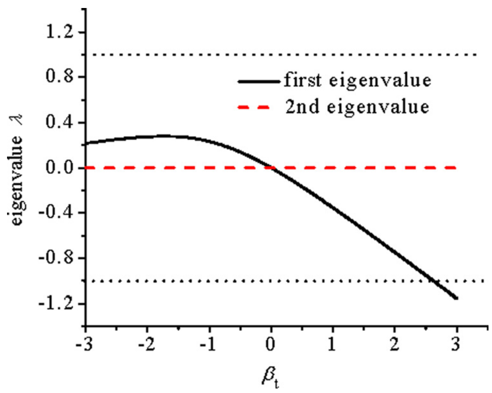


**Fig. 8** **Eigenvalues of the AMV scheme at the fixed point**

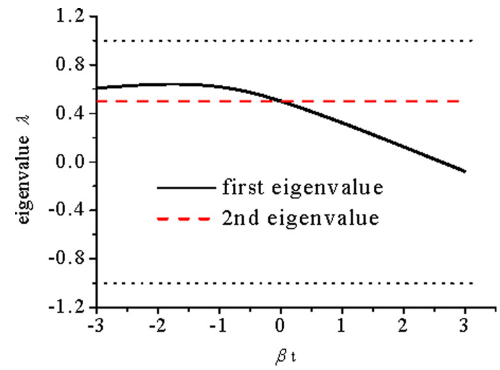


**Fig. 10** **Eigenvalues of STM scheme of the AMV formula**

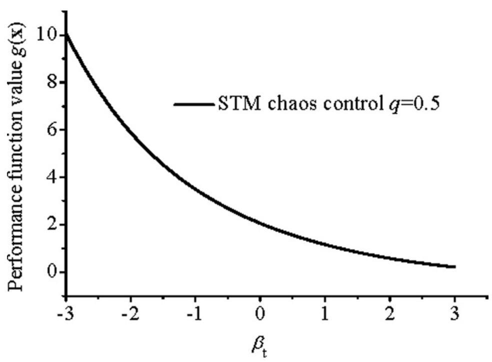


**Fig. 9** **STM control of the AMV formula**

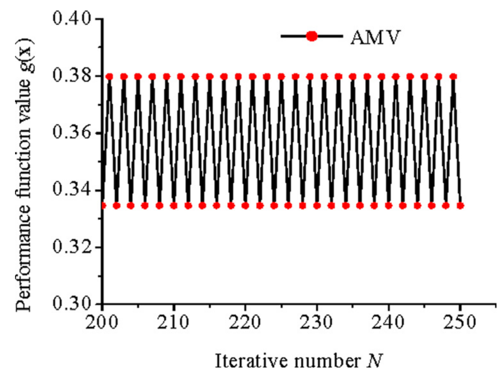


**Fig. 11** **Iterative history of the AMV formula**

$$\begin{cases} u_1^{k+1} = u_1^k + 0.5\left(-\beta_t \dfrac{0.064\exp(0.64u_1^k+2)}{\sqrt{(0.064\exp(0.64u_1^k+2))^2 + (0.056\exp(0.64u_2^k+2.9))^2}} - u_1^k\right) \\ u_2^{k+1} = u_2^k + 0.5\left(-\beta_t \dfrac{0.056\exp(0.64u_2^k+2.9)}{\sqrt{(0.064\exp(0.64u_1^k+2))^2 + (0.056\exp(0.64u_2^k+2.9))^2}} - u_2^k\right) \end{cases} \tag{17}$$

Similarly, the results of STM control for the AMV formula are illustrated in Fig. 9, and the expected stable fixed points are caught in the interval [2.618, 3]. Figure 10 displays the two eigenvalues of STM scheme of AMV formula at the fixed point with control parameter $\beta_t$. The absolute value of the first eigenvalue $\lambda_1'$ is always less than 1 in the whole interval of $\beta_t$, and the second eigenvalue at the fixed point $\lambda_2' = 1 - q = 0.5$ which can be deduced from Eq. (3) and Eq. (12). Thus, the STM scheme of AMV formula is stable in the whole range $\beta_t \in [-3, 3]$.

Figure 11 shows the iterative history of the AMV formula ($\beta_t = 3$), which generates periodic solutions. Figure 12 demonstrates the iterative history of STM control ($\mathbf{C} = \mathbf{I}$, $q = 0.5$) for the AMV formula, which captures the stable fixed point after 17 iterations.

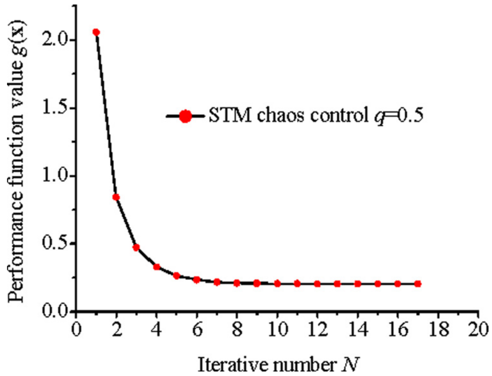


**Fig. 12 Iterative history of STM control for the AMV formula**

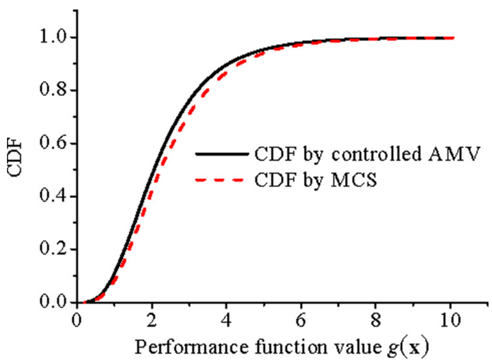


**Fig. 13 CDF of performance function**

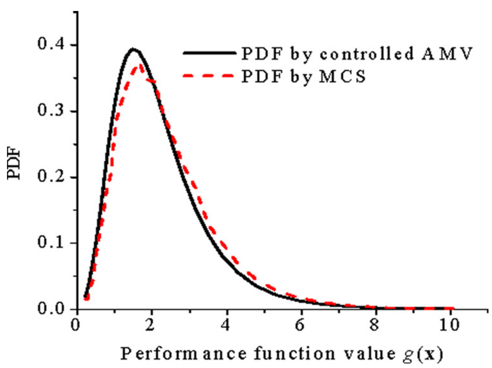


**Fig. 14 PDF of performance function**

Finally, based on the STM scheme (14) of the AMV formula, the CDF and PDF of example 2 are calculated by locating the MPTP of the performance function with the predefined target reliability index $\beta_t \in [-3, 3]$. The results are shown in Figs. 13 and 14. Also, the results from Monte Carlo simulation with $10^5$ samples are presented for comparison. It can be seen that the controlled AMV scheme of PMA compares well with the CDF and PDF of the system output as computed by the Monte Carlo approach while taking far less computational effort. In addition, the PDF of system output is an asymmetric distribution and does not obey the normal distribution, which is the probabilistic distribution of input random variables.

## 5 Convergence Control of SORA for Reliability-Based Design Optimization

The mathematical model of RBDO [4,18–20] can be generally formulated as

$$
\begin{aligned}
&\min f(\mathbf{d}) \\
&\text{s.t.} \quad P_f(g_i(\mathbf{d},\mathbf{x}) \le 0) \le P_{ti} \qquad i = 1,2,\ldots,m \\
&\qquad h_j(\mathbf{d}) \le 0 \qquad\qquad\qquad j = m+1,\ldots,M \\
&\qquad \mathbf{d}^{\mathrm{L}} \le \mathbf{d} \le \mathbf{d}^{\mathrm{U}}
\end{aligned} \tag{18}
$$

where $\mathbf{d}$ is the design variable vector, representing either deterministic physical quantities or parameters of probability distributions of the random variables (e.g., mean values or standard deviations of the random variables); $\mathbf{x}$ is the random variable vector, representing uncertain quantities; $g_i(\mathbf{d}, \mathbf{x})$ is defined as the $i$th performance function, and $g_i(\mathbf{d},\mathbf{x}) \le 0$ denotes the failure domain; $P_{ti}$ stands for the prescribed acceptable failure probability; $h_j(\mathbf{d})$ are the deterministic constraints.

It is generally acknowledged that PMA for probabilistic constraints evaluation is more efficient, stable and less dependent on probabilistic distribution types than RIA (reliability index approach) [4,18–20,26]. To enhance the computational efficiency of two-level approach in RBDO model (18), Du and Chen [13] developed the decoupled approach of SORA, which is suitable to solve the nonlinear large-scale probabilistic optimization problems [11,12]. Hereafter, SORA is selected to establish the computational formula of RBDO, while PMA is applied to evaluate the probabilistic constraints [11], as shown below

$$
\begin{aligned}
&\min f(\mathbf{d}^k) \\
&\text{s.t.} \quad \begin{cases} g_i\left(\mathbf{d}^k - \delta_i^{k-1}, \hat{\mathbf{x}}_i^{k-1}\right) \ge 0 & i = 1,\ldots,m \\ h_j\left(\mathbf{d}^k\right) \le 0 & j = m+1,\ldots,M \end{cases}
\end{aligned} \tag{19}
$$

where $k$ denotes the current optimization cycle, $\hat{\mathbf{x}}_i^{k-1}$ represents the MPTP vector in the physical space regarding the $i$th limit state obtained in the $(k-1)$th cycle, and $\delta_i^{k-1}$ stands for the shift parameter given as

$$
\begin{aligned}
\hat{\mathbf{x}}_i^{k-1} &= T(\mathbf{u}^*) \\
\delta_i^{k-1} &= \mathbf{d}^{k-1} - \hat{\mathbf{x}}_i^{k-1}
\end{aligned} \tag{20}
$$

where $\hat{\mathbf{x}}_i^{k-1}$ is the MPTP in physical space by the transformation of MPTP $\mathbf{u}^*$ in the standard normal space, which is searched by using PMA. The SORA formulation is fully deterministic and easily implemented and solved by classical optimization algorithms [11]. When the AMV iterative formula of PMA shows the numerical instability for some RBDO problems, the STM control scheme (14) is adopted to tackle this trouble.

*Example 3:* Optimization problem with highly nonlinear performance functions [4,22]

$$
\begin{aligned}
&\min \quad 2f(\mathbf{d}) = -\frac{(d_1 + d_2 - 10)^2}{30} - \frac{(d_1 - d_2 + 10)^2}{120} \\
&\text{s.t.} \quad P_f\left(g_j(\mathbf{x}) \le 0\right) \le \Phi(-\beta_t), \quad j = 1,2,3 \\
&\qquad 0 \le d_i \le 10, \quad i = 1,2
\end{aligned}
$$

where, $\mathbf{d} = [\mu(x_1), \mu(x_2)]^{\mathrm{T}}$, $x_1, x_2 \sim \mathrm{N}(5, 0.3)$, $\beta_t = 3.0$. $g_1(\mathbf{x}) = x_1^2 x_2/20 - 1$, $g_2(\mathbf{x}) = 1 - (Y-6)^2 - (Y-6)^3 + 0.6(Y-6)^4 - Z$, $g_3(\mathbf{x}) = 80/(x_1^2 + 8x_2 + 5) - 1$, $Y = 0.9063x_1 + 0.4226x_2$, $Z = 0.4226x_1 - 0.9063x_2$.

The computational results of RBDO and deterministic optimization with $\mathbf{d} = [5,\ 5]^{\mathrm{T}}$ as initial design are listed in Table 1. Table 2 demonstrates the reliabilities of three performance functions when using different optimization models. It is seen that both the method of SORA with PMA and PMA two-level obtain the incorrect optimal solutions shown in bold, because the AMV formula of PMA generates the periodic or chaotic solutions, and cannot converge and search for the stable MPTP for the second performance function $g_2(\mathbf{x})$, as scrutinized in Ref. [4]. Further, the reliabilities in bold for performance function $g_2(\mathbf{x})$ using SORA with PMA and PMA two-level do not exceed the prescribed

**Table 1 Results of RBDO and deterministic optimization for example 3**

| | Number of optimization cycles | Number of function evaluations | Optimal solution $f(d_1^*, d_2^*)$ |
|---|---|---|---|
| SORA with PMA $q=1.0$[a] | Fail to converge | | **−1.8373 (5.1498,1.7022)** |
| $q=0.5$ | 5 | 973 | −1.7228 (4.5573,1.9690) |
| $q=0.1$ | 5 | 1844 | −1.7230 (4.5570,1.9686) |
| PMA two-level $q=1.0$[a] | Fail to converge | | **−1.8340 (5.1064,1.7085)** |
| $q=0.5$ | 6 | 1701 | −1.7247 (4.5580,1.9647) |
| $q=0.1$ | 6 | 3234 | −1.7241 (4.5560,1.9661) |
| Youn et al. [22] | 6 | 187 | −1.7247 (4.5580,1.9645) |
| Deterministic optimization | 16 | 51 | −2.2917 (5.1969, 0.7045) |

[a] $q=1.0$ means no control and the original AMV formula of PMA is used.

**Table 2 Reliabilities of three performance functions with different optimization models by FORM and MCS (Note: the numbers in the bracket stands for the reliabilities by MCS)**

| | $g_1$ | $g_2$ | $g_3$ |
|---|---|---|---|
| SORA with PMA $q=1.0$ | 0.9987 (0.9986) | **0.8347** (**0.8926**) | 1.0000 (1.0000) |
| $q=0.5$ | 0.9987 (0.9986) | 0.9987 (0.9993) | 1.0000 (1.0000) |
| $q=0.1$ | 0.9987 (0.9985) | 0.9987 (0.9994) | 1.0000 (1.0000) |
| PMA two-level $q=1.0$ | 0.9986 (0.9984) | **0.8600** (**0.9111**) | 1.0000 (1.0000) |
| $q=0.5$ | 0.9987 (0.9985) | 0.9987 (0.9994) | 1.0000 (1.0000) |
| $q=0.1$ | 0.9987 (0.9985) | 0.9986 (0.9993) | 1.0000 (1.0000) |
| Youn et al. [22] | 0.9987 (0.9985) | 0.9987 (0.9993) | 1.0000 (1.0000) |
| Deterministic optimization | **0.4540** (**0.4451**) | **0.5064** (**0.5270**) | 1.0000 (1.0000) |

reliability (0.9987 for target reliability index $\beta_t = 3$), as presented in Table 2. Accordingly, before the reliability-based design optimization is solved, it is necessary to take some measures to correctly evaluate the probabilistic constraints for some problems.

Subsequently, in order to achieve the stable and attracting fixed point of performance function in which the AMV iterative scheme fails, it is desirable to apply the stability transformation formulation (14) for convergence control. Herein, the involutory matrix **C** of Eq. (14) is set as identity matrix, and the factor $q$ is taken as 0.5 and 0.1. From Table 1, it is observed that with STM convergence control ($q=0.5$), SORA with PMA converges to −1.7228 (4.5573, 1.9690) after five optimization cycles with 973 evaluations of performance functions. However, PMA two-level converges to −1.7247 (4.5580, 1.9647) after six optimization cycles with 1701 evaluations of performance functions, which takes fairly more computational cost. The optimal design and reliabilities corresponding to three performance functions are almost the same as those of Youn et al. [22]. It should be pointed out that Youn et al. [22] first performed a deterministic optimization design and then implemented RBDO based on this optimal solution, which can apparently accelerate the convergence of RBDO. If $q$ in the STM scheme of AMV formula is set as smaller value 0.1, the number of function evaluations will be increased and the stably convergent optimum design can be obtained. Summarily, SORA with PMA by STM convergence control attains the correct optimal design of RBDO problem with robust convergence and affordable computational efforts.

In addition, for the deterministic optimization of example 3, although the optimal objective is −2.2917 better than that of RBDO, the approximate reliabilities in bold for the first and second performance function by FORM are, respectively, 0.4540 and 0.5064, when the optimum design is substituted into the probabilistic constraints. It is obvious that they cannot meet the prescribed reliability requirement. Consequently, from the viewpoint of uncertainty design, the result of deterministic optimization is quite unsafe and inadmissible. For ensuring the safe optimal design, it is imperative to adopt the model and method of RBDO for engineering design.

Finally, for the case of black box functions, e.g., when constraints and/or objectives are described by FEA (finite element analysis) or CFD (computational fluid dynamics) codes, STM has the potential to tackle the numerical instabilities in RBDO. The sensitivity analysis is required to apply the difference form of implicit functions. Meantime, the original AMV formula is replaced by the STM scheme of iterative formula in searching for the MPTP.

## 6 Conclusions

Although iterative algorithms are widely used in reliability analysis and design optimization, there exist numerical instability phenomena such as periodic oscillation, bifurcation, and chaos in iterative procedures for solving some nonlinear problems.

First, the fundamental causes of chaotic dynamics for numerical instabilities of periodic oscillation and chaos of iterative solutions are exposed by detailed stability analysis of iterative procedures such as the classical Henon map and the AMV iterative formula searching for the MPTP. In the past, it was commonly recognized that the high nonlinearity of system responses leads to the nonconvergence of iterative algorithms. Actually, it is more appropriate to state that the nonlinearity of system responses formulates the nonlinear maps of iterative algorithms, leading to the numerical instabilities and nonconvergence of dynamical systems.

Moreover, as an effective, simple, and general control strategy, the stability transformation method is proposed to overcome the numerical instabilities of iterative algorithms in reliability analysis and optimal design. Several benchmark examples illustrate that STM achieves the convergence control of PMA for probabilistic analysis and SORA for reliability-based design optimization with affordable computational cost and robust convergence. In practice, STM rectifies the convergence failure of iterative algorithms while also proving convenient to implement and comprehend. Also, it is expected that STM can conquer the nonconvergence challenges of large-scale examples involving complex implicit functions for reliability analysis and optimization in structural and mechanical engineering.

Finally, it is worth pointing out that the recursive schemes in structural dynamics, heat transfer, wave propagation, and fluid dynamics possibly produce unexpected oscillating or divergent solutions. In essence, recursive schemes have the same expression as iterative schemes. Therefore, chaotic dynamics theory and STM can shed some insights into the numerical instability analysis and convergence control of these recursive schemes, and they can promote the algorithm design and development in dynamics.

## Acknowledgment

The supports of the National Natural Science Foundation of China (Grant Nos. 50978047 and 90815023), the Fundamental Research Funds for the Central Universities (Grant No. DUT11LK06), and the National Key Basic Research Development Program of China (Grant No. 2010CB832703) are much appreciated. Also, we greatly appreciate the anonymous reviewers for their insightful suggestions and comments on the early version of this paper. Finally, we thank Steven Greene of Northwestern University, USA and Yu Liu of UESTC, China for their kind help and great effort to improving the quality of this paper.

## References

[1] Yang, D. X., Li, G., and Cheng, G. D., 2006, "Convergence Analysis of First Order Reliability Method Using Chaos Theory," Comput. Struct., **84**(8–9), pp. 563–571.
[2] Yang, D. X., 2010, "Chaos Control for Numerical Instability of First Order Reliability Method," Commun. Nonlinear Sci. Numer. Simul., **15**(10), pp. 3131–3141.
[3] Yang, D. X., and Yi, P., 2009, "Chaos Control of Performance Measure Approach for Evaluation of Probabilistic Constraints," Struct. Multidiscip. Optim., **38**(1), pp. 83–92.
[4] Yi, P., and Yang, D. X., 2009, "Convergence Control of the Iterative Procedure for Performance-Measure-Based Probabilistic Structural Design Optimization," Eng. Optim., **41**(12), pp. 1145–1161.
[5] Yang, D. X., and Yang, P. X., 2010, "Numerical Instabilities and Convergence Control for Convex Approximation Methods," Nonlinear Dyn., **61**(4), pp. 605–622.
[6] Yang, D. X., and Li, G., 2009, "Chaotic Dynamics Analysis and Control of Iterative Procedure of Capacity Spectrum Method," Soil Dyn. Earthquake Eng., **29**(3), pp. 459–468.
[7] MacAuley, J. L., 1993, *Chaos, Dynamics and Fractals*, Cambridge University Press, Cambridge.
[8] Ott, E., 2002, *Chaos in Dynamical Systems*, 2nd ed., Cambridge University Press, Cambridge.
[9] Robinson, R. C., 2004, *An Introduction to Dynamical System: Continuous and Discrete*, Pearson Education, Inc, New York.
[10] Moon, F. C., 2004, *Chaotic Vibrations: An Introduction for Applied Scientists and Engineers*, John Wiley & Sons Inc, New Jersey.
[11] Aoues, Y., and Chateauneuf, A., 2010, "Benchmark Study of Numerical Methods for Reliability-Based Design Optimization," Struct. Multidiscip. Optim., **41**, pp. 277–294.
[12] Valdebenito, M. A., and Schueller, G. I., 2010, "A Survey on Approaches for Reliability-Based Optimization," Struct. Multidiscip. Optim., **42**, pp. 645–663.
[13] Du, X. P., and Chen, W., 2004, "Sequential Optimization and Reliability Assessment Method for Efficient Probabilistic Design," J. Mech. Des., **126**(2), pp. 225–233.
[14] Liu, P. L., and Kiureghian, A. D., 1991, "Optimization Algorithms for Structural Reliability," Struct. Safety, **9**, pp. 161–177.
[15] Wang, L. P., and Grandhi, R. V., 1994, "Efficient Safety Index Calculation for Structural Reliability Analysis," Comput. Struct., **52**(1), pp. 103–111.
[16] Wang, L. P., and Grandhi, R. V., 1996, "Safety Index Calculation Using Intervening Variables for Structural Reliability Analysis," Comput. Struct., **59**(6), pp. 1139–1148.
[17] Melchers, R. E., 1999, *Structural Reliability Analysis and Prediction*, 2nd ed., Ellis Horwood Limited Publishers, Chichester.
[18] Lee, J. O., Yang, Y. S., and Ruy, W. S., 2002, "A Comparative Study on Reliability-Index and Target-Performance-Based Probabilistic Structural Design Optimization," Comput. Struct., **80**, pp. 257–269.
[19] Youn, B. D., Choi, K. K., and Park, Y. H., 2003, "Hybrid Analysis Method for Reliability Based Design Optimization," J. Mech. Des., **125**(3), pp. 221–232.
[20] Du, X. P., Sudjianto, A., and Chen, W., 2004, "An Integrated Framework for Optimization Under Uncertainty Using Inverse Reliability Strategy," J. Mech. Des., **126**(7), pp. 562–570.
[21] Youn, B. D., Choi, K. K., and Du, L., 2005, "Adaptive Probability Analysis Using an Enhanced Hybrid Mean Value Method," Struct. Multidiscip. Optim., **29**, pp. 134–148.
[22] Youn, B. D., Choi, K. K., and Du, L., 2005, "Enriched Performance Measure Approach for Reliability-Based Design Optimization," AIAA J., **43**(4), pp. 874–884.
[23] Schmelcher, P., and Diakonos, F. K., 1997, "Detecting Unstable Periodic Orbits of Chaotic Dynamical Systems," Phys. Rev. Lett., **78**(25), pp. 4733–4736.
[24] Pingel, D., Schmelcher, P., and Diakonos, F. K., 2004, "Stability Transformation: A Tool to Solve Nonlinear Problems," Phys. Rep., **400**, pp. 67–148.
[25] Du, X. P., and Chen, W., 2001, "A Most Probable Point-Based Method for Efficient Uncertainty Analysis," J. Des. Manuf. Autom., **1**(1–2), pp. 47–65.
[26] Tang, Y. F., Chen, J. Q., and Wei, J. H., 2012, "A Sequential Algorithm for Reliability-Based Robust Design Optimization Under Epistemic Uncertainty," J. Mech. Des., **134**(1), 014502, pp. 1–10.